Published in final edited form as:
J Neurol. 2014 October ; 261(10): 1929–1938. doi:10.1007/s00415-014-7429-1.

A New Mutation in Gjc2 Associated with Subclinical Leukodystrophy

Charles K. Abrams[a,b], **Steven S. Scherer**[c], **Rafael Flores-Obando**[b], **Mona M Freidin**[d], **Sarah Wong**[c], **Eleonora Lamantea**[e], **Laura Farina**[e], **Vidmer Scaioli**[e], **Davide Pareyson**[e], and **Ettore Salsano**[e]

Steven S. Scherer: sscherer@mail.med.upenn.edu; Rafael Flores-Obando: rafael.flores-obando@downstate.edu; Mona M Freidin: mona.freidin@einstein.yu.edu; Sarah Wong: sarabw@mail.med.upenn.edu; Eleonora Lamantea: eleonora.lamantea@istituto-besta.it; Laura Farina: laura.farina@istituto-besta.it; Vidmer Scaioli: vidmer.scaioli@istituto-besta.it; Davide Pareyson: davide.pareyson@istituto-besta.it; Ettore Salsano: ettore.salsano@istituto-besta.it

[a]Departments of Neurology and Physiology and Pharmacology SUNY Downstate, Brooklyn, NY USA

[b]The Graduate program in Molecular and Cellular Biology, SUNY Downstate, Brooklyn, NY USA

[c]Department of Neurology, The Perelman School of Medicine at the University of Pennsylvania, Philadelphia, PA, USA

[d]Albert Einstein College of Medicine, Bronx NY, USA

[e]Fondazione IRCCS, Istituto Neurologico “C. Besta”, Milan – Italy

Abstract

Recessive mutations in *GJC2*, the gene encoding connexin 47 (Cx47), cause Pelizaeus-Merzbacher-like disease type 1 (PMLD1), a severe dysmyelinating disorder. One recessive mutation (p.Ile33Met) has been associated with a much milder phenotype - Hereditary spastic paraplegia type 44 (SPG44). Here we present evidence that a novel Arg98Leu mutation causes an even milder phenotype - a subclinical leukodystrophy. The Arg98Leu mutant forms gap junction plaques in HeLa cells comparable to wild-type Cx47, but electrical coupling was 20-fold lower in cell pairs expressing Arg98Leu than for cell pairs expressing wild-type Cx47. On the other hand, coupling between Cx47Arg98Leu and Cx43WT expressing cells did not show such reductions. Single channel conductance and normalized steady state junctional conductance-junctional voltage (G_j-V_j) relations differed only slightly from those for wild-type Cx47. Our data suggest that that the minimal phenotype in this patient results from a reduced efficiency of opening of Cx47 channels between oligodendrocyte and oligodendrocyte with preserved coupling between oligodendrocyte and astrocyte, and support a partial loss of function model for the mild Cx47 associated disease phenotypes.

Corresponding Author. Charles K Abrams, 450 Clarkson Avenue, Brooklyn NY 11203, 1 (718)-270-1270, charles.abrams@downstate.edu.

On behalf of all authors, the corresponding author states that there is no conflict of interest.

Keywords

Connexin 47; Gap junction; Pelizaeus-Merzbacher-like disease type 1 (PMLD1); Hereditary spastic paraplegia type 44 (SPG44)

Introduction

The connexins (Cxs) are a family of highly homologous integral membrane proteins, most of which can form gap junctions (GJs) that allow ions and small molecules to diffuse between adjacent cells [40]. Connexins assemble into hexameric connexons (hemichannels). Many connexins family can form functional GJs by associating with a like connexon (a homotypic junction) or a different one (a heterotypic junction). At least six connexins have been identified in CNS glia - Cx26, Cx30, and Cx43 in astrocytes, and Cx29/Cx30.3, Cx32, and Cx47 in oligodendrocytes [3]. Astrocytes can form homologous GJs (A/A GJs) comprised of Cx30:Cx30, Cx43:Cx43, and perhaps Cx26:Cx26 homotypic channels, oligodendrocytes can form homologous GJs (O/O GJs) comprised of Cx32:Cx32 and Cx47:Cx47 homotypic channels [23, 44], and oligodendrocytes can form GJs with astrocytes (O/A GJs) comprised of Cx32:Cx30 and Cx47:Cx43 [30] and perhaps Cx47:Cx30 heterotypic channels [23].

Recessive mutations in *GJC2*, the gene that encodes Cx47, are associated with Pelizaeus-Merzbacher-Like Disease type 1 (PMLD1), also known as hypomyelinating leukodystrophy type 2 (HLD2). PMLD1/HLD2/PMLD1 is phenotypically similar to Pelizaeus-Merzbacher-Disease (PMD), also known as HLD1 which is an X-linked disease caused by a subset of *PLP1* mutations. *PLP1* encodes proteolipid protein (PLP), an intrinsic membrane protein that is the major protein component of CNS myelin. PMD/HLD1 and PMLD1/HLD2 individuals have severely impaired motor development in their first year, with gait difficulties to the point of truncal instability, spasticity, pendular nystagmus, and cognitive impairment. Brain MRI of the brain shows abnormal findings in the white matter in children affected with either PMD/HLD1 or PMLD1/HLD2, which is often termed “hypomyelinating”. A subset of *PLP1* mutations result in a milder phenotype, spastic paraplegia type 2 (SPG2), characterized by a childhood late-onset myelopathy with a spastic gait.

We previously reported a family with a late-onset, progressive spastic gait disorder associated with MRI changes in the brain white matter (SPG44). This phenotype was caused by a homozygous recessive mutation in *GJC2* and is termed hereditary spastic paraplegia type 44 (SPG44) (Orthmann-Murphy et al, 2009). Unlike the PMLD1-associated mutants, Pro87Ser, Tyr269Asp, and Met283Thr, which appear to be retained in the endoplasmic reticulum and do not form functional GJs [29], the Ile33Met mutant associated with SPG44 formed gap junction plaques indistinguishable in quality and quantity from those formed by wild type (WT) Cx47. The Ile33Met mutant, however, had an altered conductance-voltage relationship to such an extent that the Cx47 cell-cell channel was predicted to be closed at all voltages. We speculated that Cx47 might have both coupling-dependent and coupling-independent functions, that the Ile33Met mutation caused a loss of function of coupling-

dependent but not coupling-independent functions, while the other mutants associated with HLD2 cause a loss of both coupling-dependant and coupling-independent functions.

Here we report a homozygous *GJC2* mutation (Arg98Leu) that was found in an adult with a subclinical leukodystrophy. In transfected cells, the Arg98Leu mutant did not affect the formation of morphologic GJ plaques, while functional studies show that pairs of cells expressing the Arg98Leu showed decreased levels of coupling. On the other hand, higher levels of coupling were seen when the Arg98Leu mutant was paired with Cx43WT, suggesting that this mutation might disrupt O/O but not O/A coupling. These results support the hypothesis that mutations that result in partial loss of function of Cx47 cause milder CNS phenotypes.

Methods

Clinical & Genetic Methods

Clinical, neuroradiological, and neurophysiological investigations were performed in a routine manner. MR Imaging was performed on a 3T scanner (Achieva; Philips Healthcare BV, Best, the Netherlands) using a 32-channel head coil. The imaging protocol included sagittal T1-weighted IR TSE images, axial T2-weighted TSE images and coronal FLAIR images. The *GJC2* gene was sequenced as previously reported (Orthmann-Murphy *et al*, 2009). The effect of amino acid substitution was evaluated for pathogenicity prediction with PolyPhen-2 (http://genetics.bwh.harvard.edu/pph2/) and SIFT (http://sift.bii.a-star.edu.sg/) software. All human studies have been approved by the appropriate ethics committee and have therefore been performed in accordance with the ethical standards laid down in the 1964 Declaration of Helsinki and its later amendments.

Analysis of transfected cells

We generated the c.293G>T (Arg98Leu) *GJC2* mutation by PCR site-directed mutagenesis using the QuikChange® II XL Site-Directed Mutagenesis Kit. (Stratagene, La Jolla, CA), from a human *GJC2* cDNA sequence in pIRES2-EGFP (GenBank accession number AF014643), using the following oligonucleotide primers (the underlined codon encodes the altered amino acid Arg98Leu): 5’- ac gcc gtg cac cTc ctg gcc cgt gc -3’; 5’- gc acg ggc cag gAg gtg cac ggc gt -3’, as previously described (Orthmann-Murphy *et al*, 2009), subcloned into pIRESpuro3 (Clontech, Mountain View, CA), and the mutation was confirmed by sequencing at the Sequencing Core of the University of Pennsylvania.

Communication-incompetent HeLa cells (gift of Dr. Bruce Nicholson) were transiently transfected to express Arg98Leu or Cx47WT as previously described (Orthmann-Murphy *et al*, 2009). Cells were plated onto 4-chamber glass slides (Nalge Nunc International, Rochester, NY), and transfected with cDNA expressing Arg98Leu or Cx47WT. After 2 days, cells were briefly fixed in 4% paraformaldehyde, and immunostained with a rabbit antiserum raised against the C-terminus of human Cx47 (diluted 1:2000), followed by a TRITC-conjugated donkey anti-rabbit antiserum secondary antibody (1:200; Jackson ImmunoResearch Laboratories, West Grove, PA), and counterstained with DAPI. The cells were imaged using TRITC filters and a 63× objective on a Leica DMR fluorescence

microscope with a Hamamatsu digital camera C4742-95 connected to a G5 Mac computer running Openlab 3.1.7, photographed under identical conditions and montaged prior to adjustment for brightness and contrast. Immunostaining was performed three times.

Human Cx43WT, Cx47WT, or Cx47Arg98Leu were subcloned into pIRES2-EGFP or pIRES2-DsRed and transiently transfected into confluent Neuro2a cells. Homotypic cell pairs were prepared by re-plating one day following transfection. For heterotypic cell pairs, transfected cells were washed and cells expressing a pIRES2-EGFP construct were mixed with cells expressing a pIRES2-DsRed construct in a 1:1 ratio. Coupling was assessed by dual whole-cell patch clamping of cell pairs 6–48 hours after re-plating as previously described [2]. Recording solutions used were as follows (in mM): pipette solution, 145 $CsCl_2$, 5 EGTA, 1.4 $CaCl_2$, and 5.0 HEPES, pH 7.2; bath solution, 150 NaCl, 4 KCl, 1 $MgCl_2$, 2 $CaCl_2$, 5 dextrose, 2 pyruvate, and 10 HEPES, pH 7.4. Heterotypic pairings between cells are shown as “connexin expressed in cell 2/connexin expressed in cell 1”; normalized junctional conductance (G_j) junctional voltage (V_j) relations were determined from isolated pairs by measuring junctional current (I_j) responses in cell 2 following 12.5 second junctional voltage pulses (from −100 mV to 100 mV in 20 mV increments) applied to cell 1, and applying Ohm’s law. Baseline junctional conductances were similarly determined by measuring instantaneous I_j responses to +/− 40 mV V_j pulses. Cytoplasmic bridges were excluded by demonstrating sensitivity of junctional conductance to application of octanol containing bath solution. For G_j-V_j plots, data was imported into Origin (Originlab, Northampton, CA), and fit to a “double Boltzmann” equation of the form:

$$G_{ss}(V)=[G_{min1}+(G_{max1}-G_{min1})/(1+e^{[A1(V-Vo1)]})]*[G_{min2}+(G_{max2}-G_{min2})/(1+e^{[A2(V-Vo2)]})]$$

where G_{ss} is the steady state junctional conductance normalized to $V_j=0$, G_{max1} and G_{max2} are the maximal and G_{min1} and G_{min2} the minimal normalized conductances for the limb reflecting the normalized residual conductances for the negative or positive limbs, and V_{01} and V_{02} are the voltage at which the conductance for the negative or positive limb is 1/2 of the difference between G_{min} and G_{max} for that limb. A_1 and A_2 are parameters which reflect the slope of the negative or positive limb of the G_j-V_j plot and are a measure of voltage sensitivity. See Abrams et al 2001 [1] for further discussion. All statistical tests were performed in GraphPad (San Diego, CA) Prism. For dual whole-cell patch clamp assays junctional conductance values were compared using the Kruskal-Wallis test with Dunn’s post-test.

RESULTS

Clinical Results

The proband was a 30-year-old Italian woman who came to our attention in April 2011 because of an abnormal brain MRI that had been obtained to evaluate one episode of malaise with skin pallor and sweating, brief partial loss of consciousness, and bladder and anal sphincter incontinence, without any evident triggering factor. There was no post-episode confusion. Some weeks later she reported a further, similar episode. Her past medical history was unremarkable. She is an only child with no known consanguinity between her

parents. She obtained a college degree, and has been actively working for the last 6 years. Her neurological examination showed only a slight postural tremor of the fingers, and bilateral palmo-mental reflexes; her deep tendon reflexes were not pathologically brisk and plantar responses were flexor. Routine laboratory investigations were normal, including a B12 level, of 290 pg/ml (normal 180–900) and normal FT3, FT4, and TSH levels. At her two-year follow up visit, she has not developed any additional symptoms or signs.

A brain MRI was obtained one year after the first MRI (Fig. 1). It showed a diffuse and subtle hyperintensity of the cerebral white matter on T2-weighted images, including the posterior limb of the internal capsules and the cerebral peduncles. On T1-weighted images, the white matter appeared normally hyperintense. This pattern is consistent with a hypomyelinating leukoencephalopathy. There were also a few focal areas of more prominent T2 hyperintensity in the periventricular and subcortical white matter, thinning of the corpus callosum, more marked at the isthmus as well as mild cerebral and cerebellar atrophy. The pons, basal ganglia, thalami, and optic radiations were normal. No interval change was found between the first and second MRI.

Clinical neurophysiology was performed (Supplementary Table 1). Motor evoked potentials (MEPs) were not replicable, but the central conduction times were normal. Visual evoked potentials (VEPs) and somatosensory evoked potentials (SEPs) revealed a slight central conduction delay, whilst in brainstem auditory evoked potentials (BAEPs), there was a marked delay in wave III and V latency and I–V interpeak time. Her electroretinogram (ERG), and electromyography with nerve conduction studies were normal (not shown). EEG showed unstable activity with photic driving response to intermittent photic stimulation. Autonomic tests were negative for cardiovascular dysautonomia.

Genetic investigations

PLP1 mutations (both deletion/duplication and point mutations) had been previously excluded. Because we had previously found a homozygous *GJC2* mutation in a patient who presented with complicated spastic paraplegia and MRI findings similar to those of this patient (Orthmann-Murphy *et al*, 2009), we sequenced this gene and found a new homozygous G to T transition at nucleotide 293 (c.293G>T) in exon 2 of the *GJC2* causing a substitution of an arginine with a leucine (p.Arg98Leu) in the Cx47 protein. The mutation was heterozygous in the healthy parents and in the public single nucleotide polymorphism databases, including dbSNP (http://www.ncbi.nlm.nih.gov/projects/SNP) and EVS (http://evs.gs.washington.edu/EVS), where it is present with a frequency of 1:12989 alleles (MAF= 0.0077%) Evolutionary comparisons by using Ensembl (www.ensembl.org) showed that the Arginine 98 is highly conserved, and the p.Arg98Leu change scored very highly for likelihood to be deleterious according to ad-hoc software for pathogenicity prediction: damaging for both Polyphen2 (p=0.911) and SIFT (score=0.02; deleterious when <0.05).

Cx47Arg98Leu forms functional GJs

To investigate whether the Arg98Leu mutant can form GJs, we transiently transfected communication–incompetent HeLa cells to express the mutant or Cx47WT. As shown in Figure 2, the Arg98Leu mutant formed GJ plaques at apposed cell borders; these cells were

indistinguishable from cells expressing of Cx47WT. We obtained similar results in three separate experiments. Similar findings were obtained using transiently transfected Neuro2a cells. (Supplementary Figure 1)

To evaluate the electrophysiological properties of the Arg98Leu mutant, Neuro2a cells were transiently transfected to express Arg98Leu mutant or Cx47WT; the transfected cells were identified by their co-expression of EGFP or dsRed. As shown in Figure 3 and Table 1, pairs of cells both expressing Arg98Leu (in the pIRES-EGFP vector) had ~20-fold reduced levels of coupling compared to cell pairs expressing Cx47WT (in the pIRES-EGFP vector). Cell pairs expressing an “empty” pIRES-EGFP vector (iG) had an even smaller (~59-fold) average conductance than cell pairs expressing Arg98Leu although the comparison of pairs expressing Arg98Leu to those expressing only empty vector did not reach statistical significance. Further, when the Arg98Leu mutant (in the pIRES-EGFP vector) was paired with cells expressing Cx47WT (in the pIRES-dsRED vector), the resulting conductances were also ~15-fold less than for pairs of cells expressing Cx47WT (one cell of each pair was in the pIRES-EGFP and the pIRES-dsRED vector) These results show that the Arg98Leu mutant is less able to form functional channels with itself or with Cx47WT.

We also investigated the electrophysiological properties of the Arg98Leu mutant with Cx43WT, its likely heterotypic partner in O/A GJs. As shown in Figure 3 and Table 1, the conductance of Arg98Leu/Cx43 heterotypic pairs was not statistically significantly different than that of the Cx47WT/Cx43WT pairs, but was statistically greater than for cell pairs expressing empty vector alone.

The Arg98Leu mutant would have to reduce the single channel conductance ~ 20-fold to account for the observed reduction in average macroscopic conductance. To assess this possibility, we examined the single channel conductance of the Arg98Leu mutant in both the homotypic configuration and when paired heterotypically with Cx43. We found that predominant unitary transitions for the homotypic channel (Figure 4a) were roughly 48 pS and estimate the residual state at about 5 pS, similar to what we and others have found for the Cx47WT homotypic channels [29, 43]. As shown in Figure 4b, the single channel conductance of the 43WT/47Arg98Leu channel shows minimal rectification, with a conductance of about 85 pS at −100 mV with respect to Cx43WT and about 75 to 80 pS at +100 mV with respect to Cx43WT. This concords with our previous report for Cx43WT/Cx47WT channels. [30].

Another possibility is that the Arg98Leu mutant shifts the voltage dependence of closure of the Cx47 hemichannel such that when two mutant hemichannels are apposed, one hemichannel from each cell-cell channel has a high probability of being in the fully or partially closed state. In such a case the mutation should have significant effects on the G_j-V_j relations. We tested this hypothesis by applying a series of junctional voltages between cell pairs, and found that the Arg98Leu mutant produces a series of time and voltage dependent currents that, except in magnitude, are virtually indistinguishable from those previously reported for Cx47 WT [29]. Furthermore, when currents such as those shown in Figure 5a are used to calculate steady state conductances (described in the Methods), the resulting G_j-V_j relation shown in Figure 5b is nearly super-imposable on that of Cx47WT.

This is reflected in the Boltzmann parameters for the Cx47 WT and Arg98Leu homotypic channels shown in Table 2. The only notable difference between the WT and the Arg98Leu mutant is a slightly lower G_{min} for the latter. Similarly, the heterotypic Cx43WT/Arg98Leu pairing shows currents and G_j-V_j relation that are similar to those seen for Cx43WT/Cx47WT; the limb of the G_j-V_j relation corresponding to the closure of the Cx47 hemichannel shows a slightly reduced G_{min} as well as a small inward shift reflecting the tendency of the Arg98Leu hemichannel to close at slightly smaller negative V_j than does the Cx47WT hemichannel. These findings are also reflected in the Boltzmann parameters shown in Table 2.

Junctional conductance, g_j is equal to $[\gamma_{s.c.}*P_o*n]$, where $\gamma_{s.c.}$ is the single channel (unitary) conductance of the Cx47 cell-cell channel, P_o is the average open probability of a Cx47 cell-cell channel, and n is the total number of junctional channels. $\gamma_{s.c.}$ of the channel formed by Arg98Leu did not differ substantially from that formed by Cx47WT. The immunostaining of Neuro2a and HeLa cells expressing Cx47WT and Cx47Arg98Leu suggests that n, the total numbers of junctional channels is similar for Cx47WT and the Cx47Arg98Leu mutant.

The most straightforward explanation for reduced g_j is that the Arg98Leu mutant reduces the P_o of the Cx47 cell-cell channel. Shifts in the Po-V_j relationship (a common mechanism for reduced or absent coupling by mutant forms of connexins) would be reflected in alteration of Gj-V_j relations [1, 28, 31]) but G_j-V_j relations for Cx47Arg98Leu/Cx47Arg98Leu and Cx43WT/Cx47Arg98Leu pairings were nearly indistinguishable from those for Cx47WT/Cx47WT or Cx43WT/Cx47WT pairings, respectively.

Reducing the mean open time of active channels or increasing the mean closed times would both reduce P_o, but neither one seems likely. First, although we did not formally assess these parameters, no qualitative differences were seen in recordings from cells pairs where unitary transitions could be observed; for alterations in these parameters to account for the 20-fold reduction in overall conductance the effects would have to be very dramatic. Secondly, if the mutant simply induced a change P_o, one would expect that the distributions of measured conductances for the Arg98Leu mutant pairs would be scaled to the ratio of P_o(Arg98Leu)/P_o(WT), leading to identical coefficients of variation and similar failure rates. (Failure rate here is defined as the proportion of cells showing no functional coupling). However, this is not the case. The coefficient of variation is 4.14 for the mutant and 1.04 for Cx47WT and the failure rate for the mutant (16/30 vs 1/13 for the WT) is significantly higher (p=0.004 by Fisher's exact test). Reductions in P_o may also arise from reduced efficiency of channel opening, a possibility we deal with in more detail in the Discussion.

DISCUSSION

Hypomyelinating leukodystrophies encompass a variety of rare diseases with different pattern of inheritance, and clinical onset usually during infancy or childhood. They include PMD and PMLD1, *alias* named HLD1 and HLD2, respectively, and other entities characterized by hypomyelination on brain MRI and congenital cataract (HLD5), extrapyramidal symptoms and atrophy of the basal ganglia and cerebellum (HLD6), hypogonadotropic hypogonadism and hypodontia (HLD7 and HLD8) [16]. A small subset

of the inherited spastic paraplegias (SPG) are caused by mutations in some of the same genes - *PLP1* (SPG2) and *GJC2* (SPG44). These phenotypes may represent milder consequences of hpomyelination; alternatively they may reflect axonal loss in response to abnormal myelination rather than demyelination *per se* [12]. The patient we report had a subclinical hypomyelinating leukodystrophy that is associated with a novel homozygous mutation in the *GJC2*. The Arg98Leu mutant can form functional channels that have mildly altered biophysical features. A subtle perturbation of Cx47 channels fits the minimal phenotype of the patient and thus extends the possible genotype-phenotype correlation that we previously suggested [31] – complete loss-of-function mutations cause PMLD1/HLD2, partial loss-of-function mutations cause SPG44, and the mildly altered function cause a subclinical leukodystrophy. Homozygous promoter mutations in *GJC2* result in a phenotype between PMLD1/HLD2 and SPG44 [25, 32]. Promoter mutations may simply reduce expression of Cx47 leading to partial loss of function. However, experiments to determine effects of these mutations on expression levels have yielded conflicting results. [9, 32]

CMT1X, the most common X-linked form of the inherited peripheral neuropathy Charcot-Marie–Tooth disease, is caused by mutations in connexin 32, a gap junction protein expressed in the Schwann cell, the myelinating cell of the peripheral nervous system and in oligodendrocytes in the central nervous system. Many patients with CMT1X have subclinical abnormalities of VERs and BAERs [26, 27]; a few patients have static, potentially asymptomatic white matter abnormalities and/or static corticospinal tract dysfunction [3]. The clinical phenotypes in these cases appear to have some overlap with the milder forms of Cx47 associated disease and may reflect a similar underlying pathology. This is an appealing idea since at least one study [44] suggests that loss of Cx32 would have greater impact on loss of oligodendrocyte-oligodendrocyte than on oligodendrocyte-astrocyte coupling as is predicted to be the case with the Cx47R98L mutation. However the results from another group do not show a significant role for Cx32 in oligodendrocyte-oligodendrocyte coupling. In addition some patients with CMT1X suffer from acute, transient neurological presentations accompanied by transient white matter abnormalities on MRI, often triggered by a stressor such as high altitude or fever.[15, 19, 34, 38] To the best of our knowledge this phenotype is not seen in patients with mutations in Cx47.

Given the unique clinical phenotype of patients expressing the R98L mutation, we performed functional *in vitro* studies to examine the functional effects of the mutation. Though the mutant formed normal appearing gap junction plaques, cell pairs expressing the Arg98Leu mutant had reduced levels of total junctional conductance. As noted in the results section, the data suggest that the reductions in P_O, the open probability of the R98L homotypic channel, arise due to reduced reduced efficiency of channel function, a concept first investigated by Bukauskas and colleagues [8]. They recorded coupling between cells that were joined by gap junction plaques (formed by Cx43-EGFP fusion proteins) and found no junctional coupling until there were about 400 cell-cell channels. Thus, only about 0.25% of the channels within that plaque were open at any given time. Comparisons of numbers of channels on Mauthner cell club endings observed by freeze fracture electron microscopy to numbers calculated from measured junctional conductances suggest that about 15% of channels at those junctions are active [35]. This is a much higher number than that seen by

Bukauskas et al [8] but is still only a small fraction of total channels available at the club endings. We propose that the Arg98Leu mutation reduces the efficiency of channel function to ~1/20th that of Cx47WT. It is possible that a small part of the reduction in function may also be due to other mechanisms outlined above. What might account for a reduced efficiency of gating in the Arg98Leu mutant? Gating of connexins is generally conceived of as a voltage dependant process. However, the transition from closed channel to open channel may have both voltage dependent and voltage independent steps. In the case of the Arg98Leu mutant the voltage independent barrier to opening may be increased while the voltage dependent barrier, reflected in the wild-type like G_j-V_j relations, is essentially unaltered.

Interestingly, the apparent reduced efficiency of the Cx47Arg98Leu/Cx47Arg98Leu homotypic channel seems, at least in part, corrected by heterotypic pairing of Cx47Arg98Leu with Cx43WT. As shown in Figure 4, Cx47Arg98Leu/Cx47Arg98Leu pairs express at a level that is significantly higher than for pairs expressing Cx47Arg98Leu/ Cx47Arg98Leu homotypic channels. Coupling between oligodendrocytes is mediated, at least in part by Cx47 homotypic channels [23, 44], while oligodentrocyte-astrocyte coupling is partially dependent on Cx47/Cx43 heterotypic channels [30]. Thus, we suggest that the phenotype seen in this patient may reflect the effects of reduced oligodendrocyte-oligodendrocyte coupling with preservation of oligodendrocyte-astrocyte coupling. One possible explanation for this disparity is that heterotypic pairing of Cx47 with Cx43 stabilizes the mutant in a way that is not the case with pairing of homotypically paired Cx47. Recent work by May and collegues [10] suggests one possible molecular mechanism for this stabilization. May et al found that in a mouse lacking Cx32 expression in all cells and Cx43 expression in astrocytes, thus eliminating heterotypic O/A coupling, levels of Cx47 expression were dramatically reduced, and that this reduction was accompanied by reduced phosphorylation of Cx47. In contrast mice lacking Cx32 expression but expressing a non-channel forming mutant of Cx43 showed a normal magnitude and phosphorylation pattern of Cx47. They suggest that formation of heterotypic docking of Cx47/Cx43, even without channel formation, may induce conformational changes in Cx47 which allow for phosphorylation of Cx47, which in turn stabilizes the protein. Though our experiments on the Cx47R98L mutant were performed in an exogenous expression system where both homotypic and heterotypic wild–type channels produce robust coupling, the general principle of enhanced stabilization of the Cx47R98L mutant in the heterotypic over the homotypic configuration may apply here as well.

What might account for the clinical phenotype in patients with the Cx47R98L mutation? It is well accepted that connexins provide metabolic or electrical coupling pathways between cells [21]. Glial coupling creates a dynamic, regulated cellular network [13]. One possible role for such a network is cell signaling, for example via enhanced propagation of Ca^{2+} waves. (See [37] for more detail.) Glial gap junctions may provide reflexive coupling between adjacent loops of non-compact myelin [5]. Work by Menichella et al. [24] supports the hypothesis that oligodendrocyte Cx32 and Cx47 are involved in spatial buffering of K^+ during neuronal activity. Loss of one or more of these functions could have detrimental effects on myelination.

Supplementary Material

Refer to Web version on PubMed Central for supplementary material.

Acknowledgements

This work was supported by the National Multiple Sclerosis Society (C.K.A. and S.S.S.) and National Institutes of Health (NIH) grants: NS055284 (to S.S.S.), and NS067404 (to C.K.A.) and the Pierfranco and Luisa Mariani Foundation, Italy (E.L.)

REFERENCES

1. Abrams CK, Freidin MM, Verselis VK, Bennett MV, Bargiello TA. Functional alterations in gap junction channels formed by mutant forms of connexin 32: evidence for loss of function as a pathogenic mechanism in the X-linked form of Charcot-Marie-Tooth disease. Brain Res. 2001; 900:9–25. [PubMed: 11325342]
2. Abrams CK, Islam M, Mahmoud R, Kwon T, Bargiello TA, Freidin MM. Functional requirement for a highly conserved charged residue at position 75 in the gap junction protein connexin 32. J Biol Chem. 2013; 288:3609–3619. [PubMed: 23209285]
3. Abrams CK, Scherer SS. Gap junctions in inherited human disorders of the central nervous system. Biochim Biophys Acta. 2012; 1818:2030–2047. [PubMed: 21871435]
4. Anand G, Maheshwari N, Roberts D, Padeniya A, Hamilton-Ayers M, van der Knaap M, Fratter C, Jayawant S. X-linked hereditary motor sensory neuropathy (type 1) presenting with a stroke-like episode. Developmental medicine and child neurology. 2010; 52:677–679. [PubMed: 20491857]
5. Balice-Gordon RJ, Bone LJ, Scherer SS. Functional gap junctions in the schwann cell myelin sheath. J Cell Biol. 1998; 142:1095–1104. [PubMed: 9722620]
6. Basri R, Yabe I, Soma H, Matsushima M, Tsuji S, Sasaki H. X-linked Charcot-Marie-Tooth disease (CMTX) in a severely affected female patient with scattered lesions in cerebral white matter. Internal medicine (Tokyo, Japan). 2007; 46:1023–1027.
7. Bort S, Nelis E, Timmerman V, Sevilla T, Cruz-Martinez A, Martinez F, Millan JM, Arpa J, Vilchez JJ, Prieto F, Van Broeckhoven C, Palau F. Mutational analysis of the MPZ, PMP22 and Cx32 genes in patients of Spanish ancestry with Charcot-Marie-Tooth disease and hereditary neuropathy with liability to pressure palsies. Hum Genet. 1997; 99:746–754. [PubMed: 9187667]
8. Bukauskas FF, Jordan K, Bukauskiene A, Bennett MV, Lampe PD, Laird DW, Verselis VK. Clustering of connexin 43-enhanced green fluorescent protein gap junction channels and functional coupling in living cells. Proc Natl Acad Sci U S A. 2000; 97:2556–2561. [PubMed: 10706639]
9. Combes P, Kammoun N, Monnier A, Gonthier-Guéret C, Giraud G, Bertini E, T C, Fakhfakh F, Boespflug-Tanguy O, Vaurs-Barrière C. Relevance of GJC2 promoter mutation in Pelizaeus-Merzbacher-like disease. Ann Neurol. 2012; 71:146-. [PubMed: 21246605]
10. Freidin M, Asche S, Bargiello TA, Bennett MV, Abrams CK. Connexin 32 increases the proliferative response of Schwann cells to neuregulin-1 (Nrg1). Proc Natl Acad Sci U S A. 2009; 106:3567–3572. [PubMed: 19218461]
11. Fusco C, Frattini D, Pisani F, Spaggiari F, Ferlini A, Della Giustina E. Coexistent central and peripheral nervous system involvement in a Charcot-Marie-Tooth syndrome X-linked patient. J Child Neurol. 2010; 25:759–763. [PubMed: 20382840]
12. Garbern JY, Yool DA, Moore GJ, Wilds IB, Faulk MW, Klugmann M, Nave KA, Sistermans EA, van der Knaap MS, Bird TD, Shy ME, Kamholz JA, Griffiths IR. Patients lacking the major CNS myelin protein, proteolipid protein 1, develop length-dependent axonal degeneration in the absence of demyelination and inflammation. Brain. 2002; 125:551–561. [PubMed: 11872612]
13. Giaume C, Koulakoff A, Roux L, Holcman D, Rouach N. Astroglial networks: a step further in neuroglial and gliovascular interactions. Nat Rev Neurosci. 2010; 11:87–99. [PubMed: 20087359]
14. Halbrich M, Barnes J, Bunge M, Joshi C. A V139M mutation also causes the reversible CNS phenotype in CMTX. The Canadian journal of neurological sciences. 2008; 35:372–374. [PubMed: 18714809]

15. Hanemann CO, Bergmann C, Senderek J, Zerres K, Sperfeld AD. Transient, recurrent, white matter lesions in X-linked Charcot-Marie-Tooth disease with novel connexin 32 mutation. Arch Neurol. 2003; 60:605–609. [PubMed: 12707076]
16. Hobson GM, Garbern JY. Pelizaeus-Merzbacher disease, Pelizaeus-Merzbacher-like disease 1, and related hypomyelinating disorders. Semin Neurol. 2012; 32:62–67. [PubMed: 22422208]
17. Isoardo G, Di Vito N, Nobile M, Benetton G, Fassio F. X-linked Charcot-Marie-Tooth disease and progressive-relapsing central demyelinating disease. Neurology. 2005; 65:1672–1673. [PubMed: 16301507]
18. Karadima G, Panas M, Floroskufi P, Kalfakis N, Vassilopoulos D. Four novel connexin 32 mutations in X-linked Charcot-Marie-Tooth disease with phenotypic variability. J Neurol. 2006; 253:263–264. [PubMed: 16096811]
19. Kassubek J, Bretschneider V, Sperfeld AD. Corticospinal tract MRI hyperintensity in X-linked Charcot-Marie-Tooth Disease. J Clin Neurosci. 2005; 12:588–589. [PubMed: 16051098]
20. Kleopa KA, Zamba-Papanicolaou E, Alevra X, Nicolaou P, Georgiou DM, Hadjisavvas A, Kyriakides T, Christodoulou K. Phenotypic and cellular expression of two novel connexin32 mutations causing CMT1X. Neurology. 2006; 66:396–402. [PubMed: 16476939]
21. Kumar NM, Gilula NB. The gap junction communication channel. Cell. 1996; 84:381–388. [PubMed: 8608591]
22. Lee MJ, Nelson I, Houlden H, Sweeney MG, Hilton-Jones D, Blake J, Wood NW, Reilly MM. Six novel connexin32 (GJB1) mutations in X-linked Charcot-Marie-Tooth disease. Journal of neurology, neurosurgery, and psychiatry. 2002; 73:304–306.
23. Magnotti LM, Goodenough DA, Paul DL. Functional heterotypic interactions between astrocyte and oligodendrocyte connexins. Glia. 2011; 59:26–34. [PubMed: 21046554]
24. Menichella DM, Majdan M, Awatramani R, Goodenough DA, Sirkowski E, Scherer SS, Paul DL. Genetic and physiological evidence that oligodendrocyte gap junctions contribute to spatial buffering of potassium released during neuronal activity. J Neurosci. 2006; 26:10984–10991. [PubMed: 17065440]
25. Nezu A, Kimura S, Uehara S, Osaka H, Kobayashi T, Haraguchi M, Inoue K, Kawanishi C. Pelizaeus-Merzbacher-like disease: female case report. Brain Dev. 1996; 18:114–118. [PubMed: 8733901]
26. Nicholson G, Corbett A. Slowing of central conduction in X-linked Charcot-Marie-Tooth neuropathy shown by brain stem auditory evoked responses. Journal of neurology, neurosurgery, and psychiatry. 1996; 61:43–46.
27. Nicholson GA, Yeung L, Corbett A. Efficient neurophysiologic selection of X-linked Charcot-Marie-Tooth families: ten novel mutations. Neurology. 1998; 51:1412–1416. [PubMed: 9818870]
28. Oh S, Ri Y, Bennett MV, Trexler EB, Verselis VK, Bargiello TA. Changes in permeability caused by connexin 32 mutations underlie X- linked Charcot-Marie-Tooth disease. Neuron. 1997; 19:927–938. [PubMed: 9354338]
29. Orthmann-Murphy JL, Enriquez AD, Abrams CK, Scherer SS. Loss-of-function GJA12/Connexin47 mutations cause Pelizaeus-Merzbacher-like disease. Mol Cell Neurosci. 2007; 34:629–641. [PubMed: 17344063]
30. Orthmann-Murphy JL, Freidin M, Fischer E, Scherer SS, Abrams CK. Two distinct heterotypic channels mediate gap junction coupling between astrocyte and oligodendrocyte connexins. J Neurosci. 2007; 27:13949–13957. [PubMed: 18094232]
31. Orthmann-Murphy JL, Salsano E, Abrams CK, Bizzi A, Uziel G, Freidin MM, Lamantea E, Zeviani M, Scherer SS, Pareyson D. Hereditary spastic paraplegia is a novel phenotype for GJA12/GJC2 mutations. Brain. 2009; 132:426–438. [PubMed: 19056803]
32. Osaka H, Hamanoue H, Yamamoto R, Nezu A, Sasaki M, Saitsu H, Kurosawa K, Shimbo H, Matsumoto N, Inoue K. Disrupted SOX10 regulation of GJC2 transcription causes Pelizaeus-Merzbacher-like disease. Ann Neurol. 2010; 68:250–254. [PubMed: 20695017]
33. Panas M, Karadimas C, Avramopoulos D, Vassilopoulos D. Central nervous system involvement in four patients with Charcot-Marie-Tooth disease with connexin 32 extracellular mutations. Journal of neurology, neurosurgery, and psychiatry. 1998; 65:947–948.

34. Paulson HL, Garbern JY, Hoban TF, Krajewski KM, Lewis RA, Fischbeck KH, Grossman RI, Lenkinski R, Kamholz JA, Shy ME. Transient central nervous system white matter abnormality in X-linked Charcot-Marie-Tooth disease. Ann Neurol. 2002; 52:429–434. [PubMed: 12325071]
35. Pereda AE, Rash JE, Nagy JI, Bennett MV. Dynamics of electrical transmission at club endings on the Mauthner cells. Brain research Brain research reviews. 2004; 47:227–244. [PubMed: 15572174]
36. Rosser T, Muir J, Panigrahy A, Baldwin EE, Boles RG. Transient leukoencephalopathy associated with X-linked Charcot-Marie-Tooth disease. J Child Neurol. 2010; 25:1013–1016. [PubMed: 20472869]
37. Scemes E, Giaume C. Astrocyte calcium waves: what they are and what they do. Glia. 2006; 54:716–725. [PubMed: 17006900]
38. Schelhaas HJ, Van Engelen BG, Gabreels-Festen AA, Hageman G, Vliegen JH, Van Der Knaap MS, Zwarts MJ. Transient cerebral white matter lesions in a patient with connexin 32 missense mutation. Neurology. 2002; 59:2007–2008. [PubMed: 12499506]
39. Siskind C, Feely SM, Bernes S, Shy ME, Garbern JY. Persistent CNS dysfunction in a boy with CMT1X. J Neurol Sci. 2009; 279:109–113. [PubMed: 19193385]
40. Sohl G, Willecke K. An Update on Connexin Genes and their Nomenclature in Mouse and Man. Cell Commun Adhes. 2003; 10:173–180. [PubMed: 14681012]
41. Srinivasan J, Leventer RJ, Kornberg AJ, Dahl HH, Ryan MM. Central Nervous System Signs in X-Linked Charcot-Marie-Tooth Disease After Hyperventilation. Pediatr Neurol. 2008; 38:293–295. [PubMed: 18358413]
42. Taylor RA, Simon EM, Marks HG, Scherer SS. The CNS phenotype of X-linked Charcot-Marie-Tooth disease: more than a peripheral problem. Neurology. 2003; 61:1475–1478. [PubMed: 14663027]
43. Teubner B, Odermatt B, Guldenagel M, Sohl G, Degen J, Bukauskas F, Kronengold J, Verselis VK, Jung YT, Kozak CA, Schilling K, Willecke K. Functional expression of the new gap junction gene connexin47 transcribed in mouse brain and spinal cord neurons. J Neurosci. 2001; 21:1117–1126. [PubMed: 11160382]
44. Wasseff SK, Scherer SS. Cx32 and Cx47 mediate oligodendrocyte: Astrocyte and oligodendrocyte:oligodendrocyte gap junction coupling. Neurobiol dis. 2011; 42:506–513. [PubMed: 21396451]

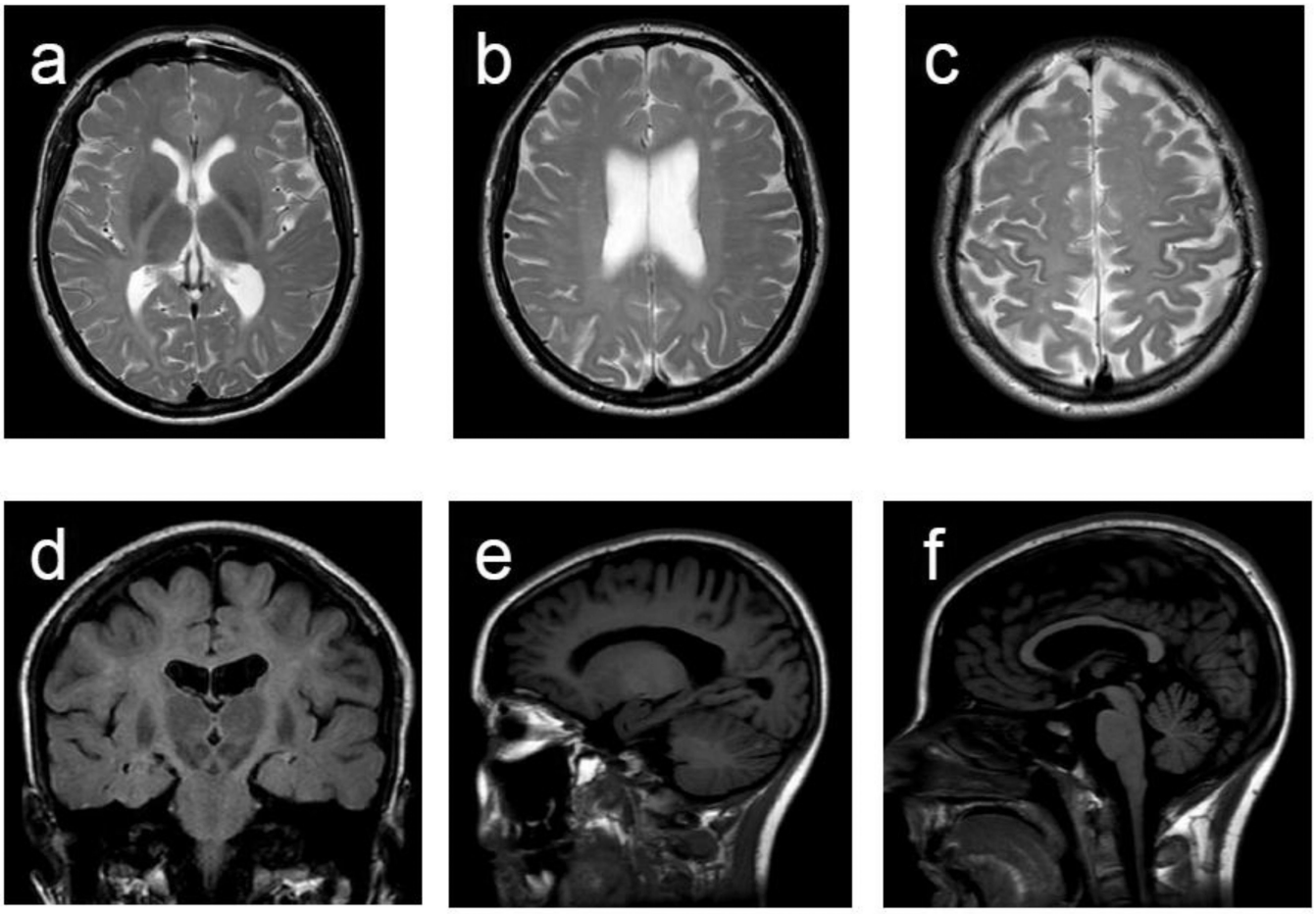

Figure 1. Brain MRI

a, b, c, d. Diffuse hyperintensity in the subcortical, lobar, and periventricular white matter including posterior limb of the internal capsules (a & d) and cerebral peduncles (d) is seen. The signal abnormalities were slightly more marked in the precentral and postcentral gyri (c). **e.** Normal white matter signal intensity is noted on T1-weighted image. **f.** Thinning of the corpus callosum, more marked posteriorly, is present. In all the images enlarged ventricles and sulci are noted. a, b, and c are axial T2-weighted images, d is a coronal FLAIR image, and e and f are sagittal T1-weighted images.

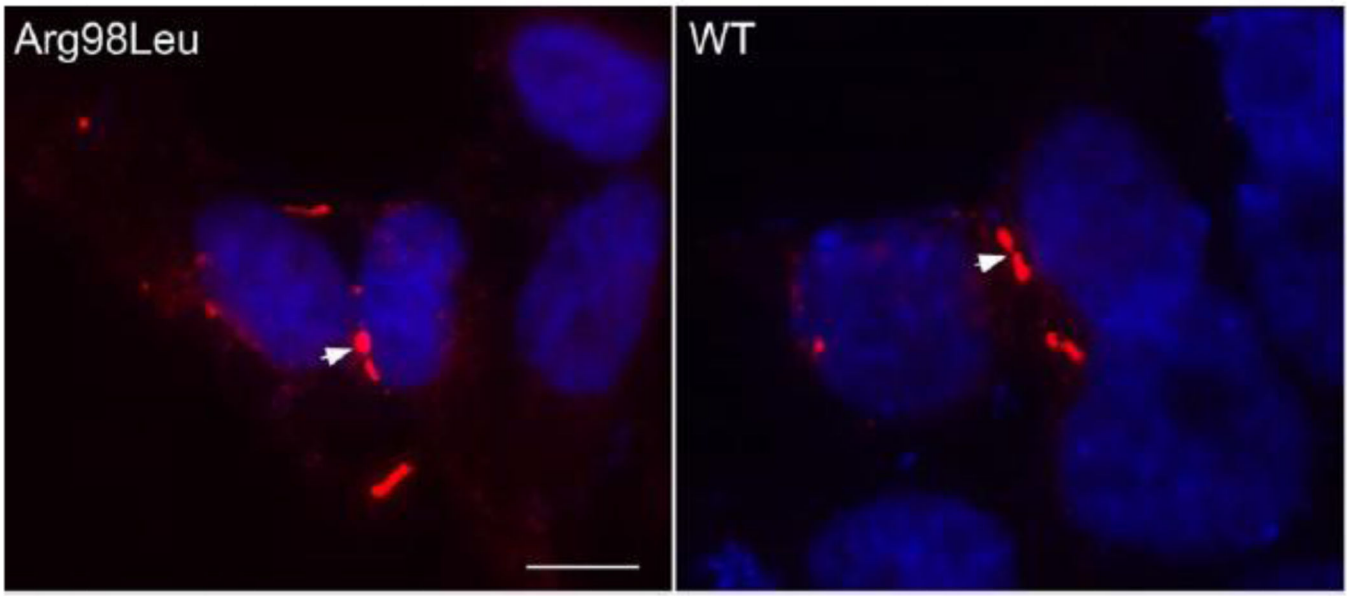

Figure 2. The Arg98Leu mutant forms GJ plaques

These are images of HeLa cells that were transiently transfected to express Arg98Leu or wild-type Cx47 (WT), immunostained with a rabbit antiserum against human Cx47 and counterstained with DAPI. Both Arg98Leu and Cx47WT form GJ plaques (arrowheads) at apposed cell membranes. Scale bar: 10 μm

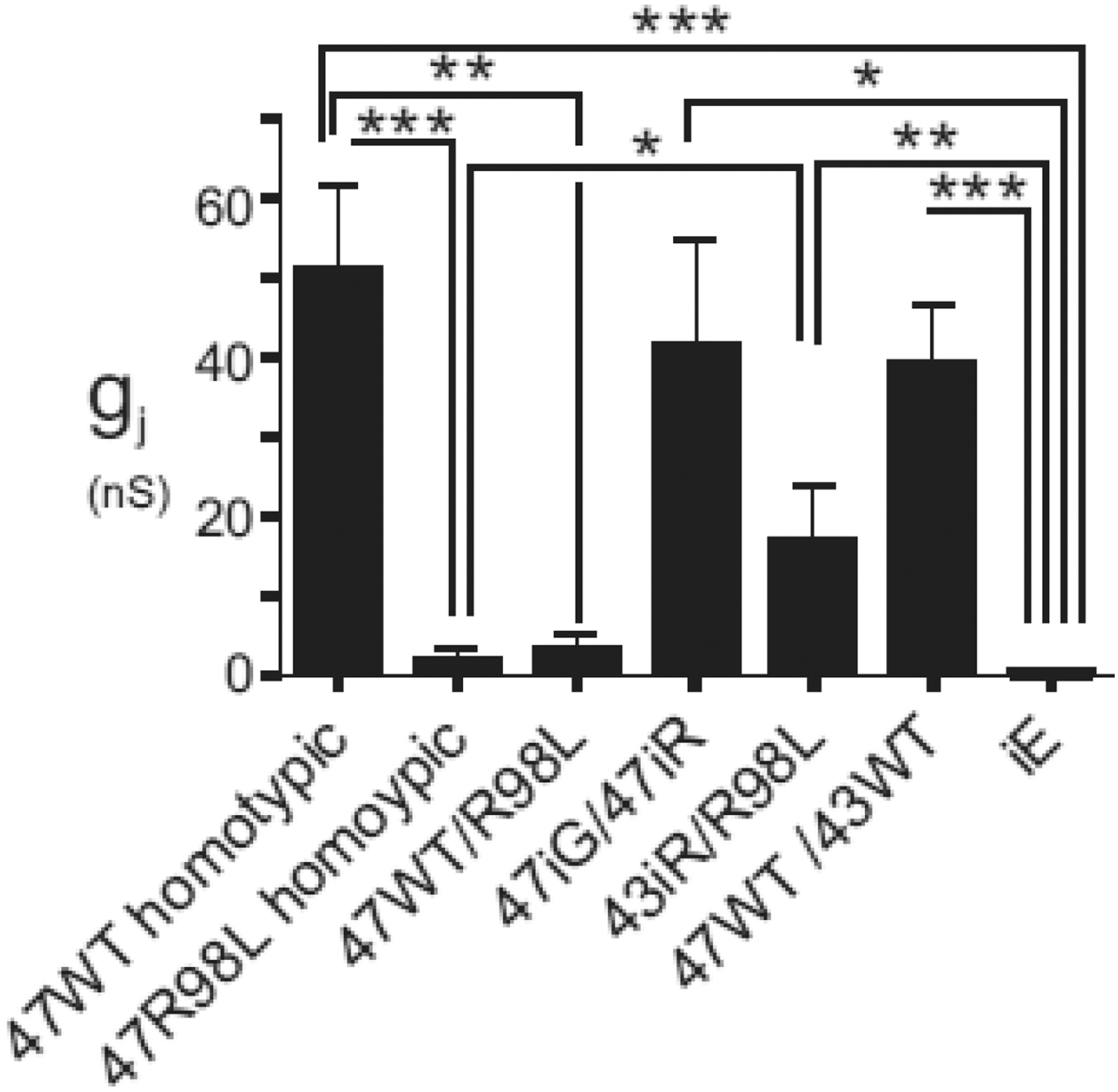

Figure 3. Junctional coupling for Cx47WT, and Cx47Arg98Leu (R98L) mutant and controls

Neuro2a cells were transiently transfected using pIRES-EGFP (iG) or pIRESdsRed (iR) vectors to express wild-type Cx47WT (47WT), Cx47Arg98Leu (R98L), or Cx43WT (43WT). Homotypic R98L/R98L and heterotypic R98L/47WT pairs show substantially lower levels of functional coupling than seen for 47WT/47WT homotypic pairs. The coupling for the R98L/43WT heterotypic pairings is not significantly different than for the 47WT/43WT pairings; R98L/43WT is statistically significantly different than the vector only controls.* $p<0.05$, ** $p<0.01$, *** $p<0.001$.

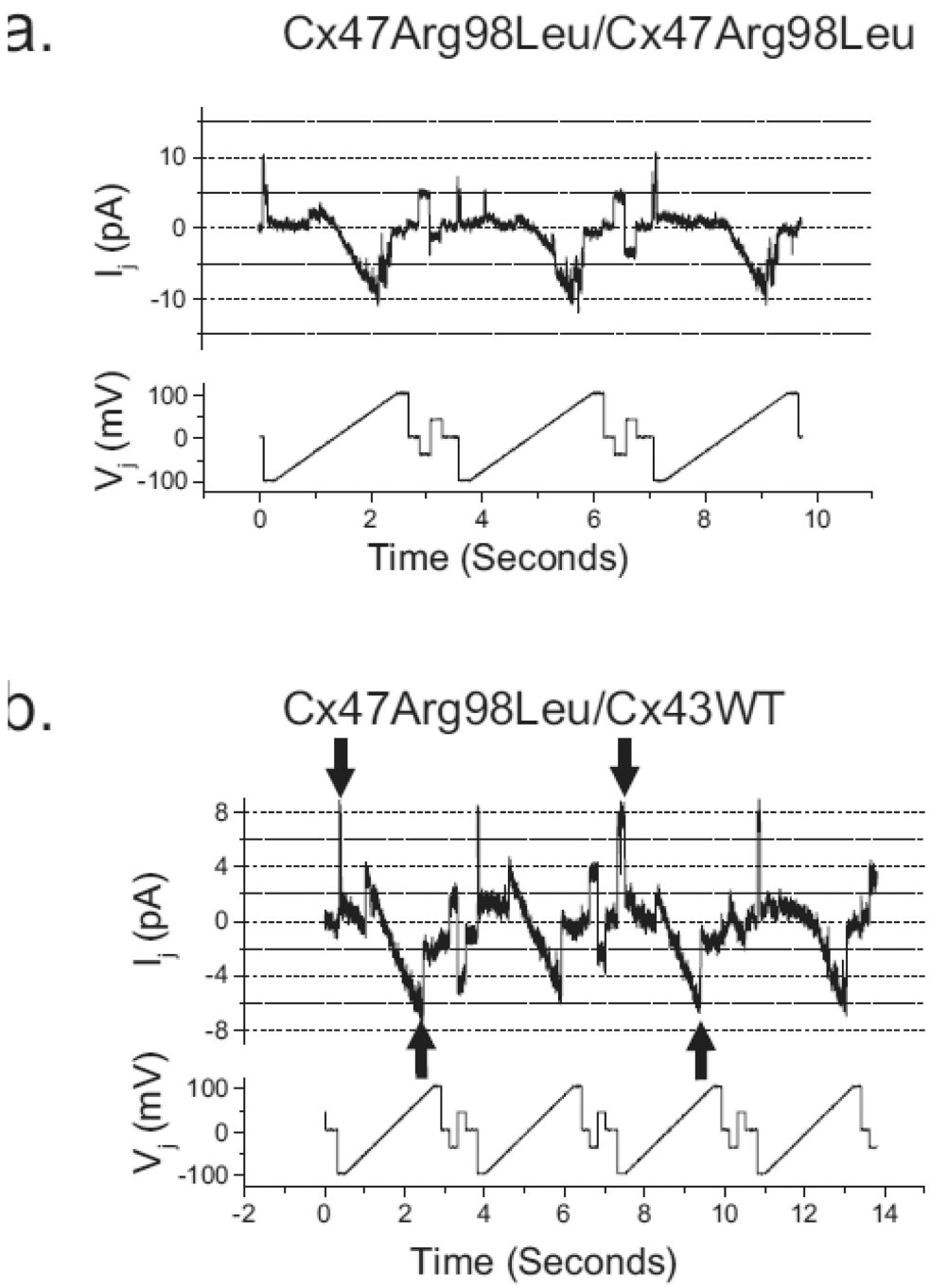

Figure 4. Single channel recordings of Cx47Arg98Leu/Cx47Arg98Leu homotypic and Cx47Arg98Leu/Cx43WT heterotypic channels

The unitary conductance transitions for homotypic and Cx43WT/Cx47Arg98Leu heterotypic channels were determined by applying voltage ramps (V_j bottom panels) from +100 to −100 mV to cell 1 (expressing Cx47Arg98Leu or Cx43WT) of poorly coupled cell pairs, and measuring the junctional currents (I_j, upper panels) in cell 2 (expressing Cx47Arg98Leu). **a.** The conductance the of Cx47Arg98Leu/Cx47Arg98Leu channel shows predominant unitary transitions for the homotypic channel of about 48 pS, similar to what

we and others have found for the Cx47WT homotypic channels [29, 43]. The residual state is difficult to estimate with certainty because the number of active channels is not known with certainty but appears to be about 5 pS. **b.** The single channel conductance of the Cx47Arg98Leu/Cx43WT channel shows minimal rectification, with a conductance of about 85 pS at −100 mV with respect to Cx43WT and about 75 to 80 pS at +100 mV with respect to Cx43WT. Gating of the Cx43 hemichannel likely accounts for closures with negative V_j (downgoing arrows) whereas gating of the Cx47 hemichannel likely accounts for closures when the polarity of V_j is reversed (upgoing arrows), because both of these hemichannels have negative gating polarities. Traces were filtered at 150 Hz (a) and 200 Hz (b).

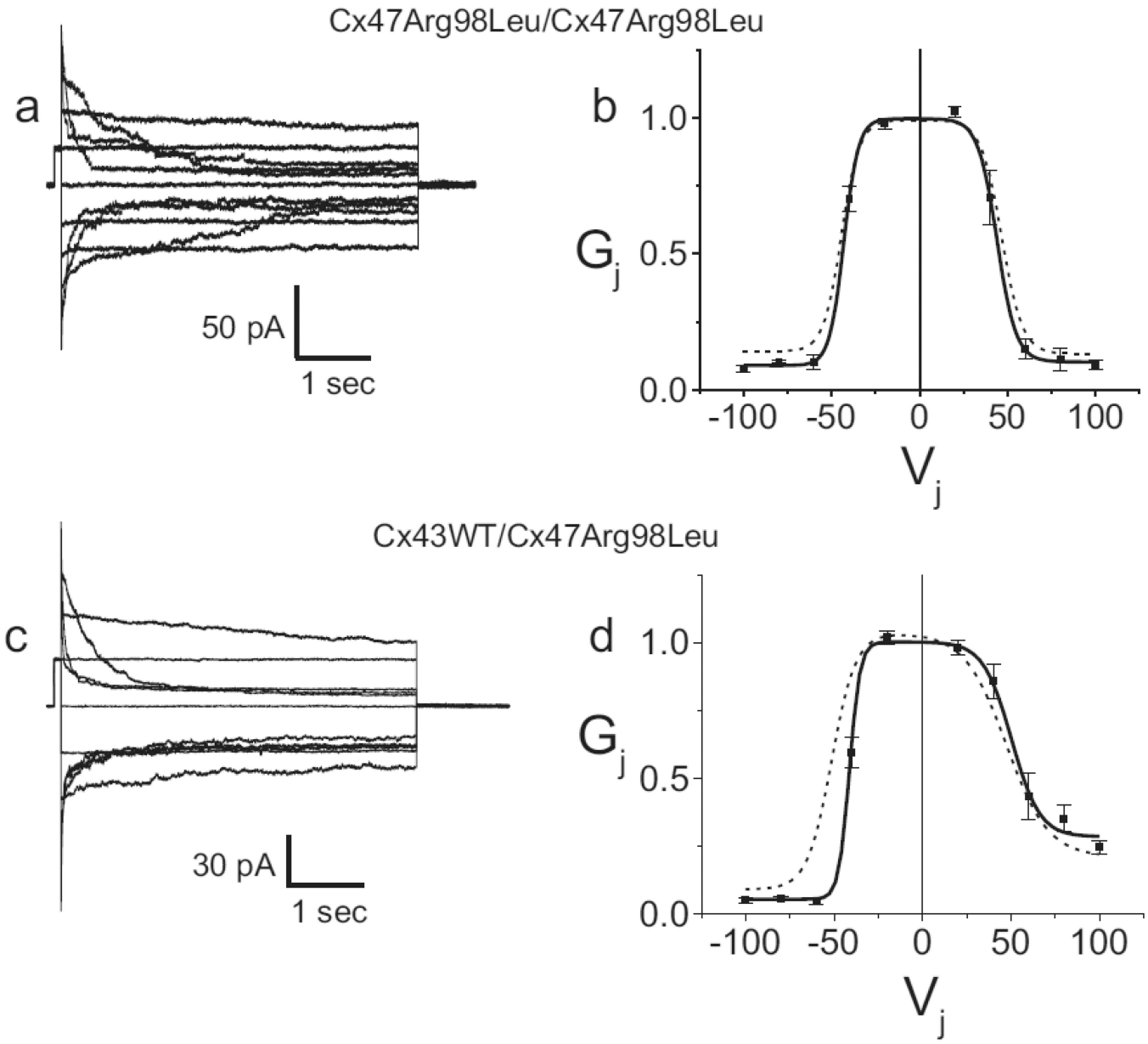

Figure 5. Representative current traces (a, c) and G_j-V_j relations (b, d), for Arg98Leu expressed in Neuro2a cells and paired homotypically or heterotypically with Cx43 WT

a. Macroscopic junctional currents for homotypically paired cells expressing the Cx47Arg98Leu mutant are similar to those seen for Cx47WT. **b.** Steady state G_j-V_j relations for homotypically paired cells expressing the Arg98Leu mutant are similar to those seen for Cx47WT, though the Arg98Leu mutant shows a slightly decreased G_{min}. **c.** Macroscopic junctional currents between heterotypic cells pairs in the Cx43WT/Cx47Arg98Leu configuration are similar to those seen for Cx43WT/Cx47WT. **d.** Steady state G_j-V_j relations for heterotypic Cx43WT/Cx47Arg98Leu junctions are, for the most part, similar to those seen for Cx43WT/Cx47WT junctions though the negative limb of the Cx43WT/Arg98Leu G_j-V_j relation (corresponding to the closure of the Cx47 hemichannel) shows a modest inward shift (indicating closure at smaller V_j) and a slightly decreased G_{min}

compared to that for Cx43WT/Cx47WT. Filled squares are average normalized conductances. Error bars represent SEM. Solid lines are Boltzmann fits to the steady state Cx47Arg98Leu/Cx47Arg98Leu and Cx43WT/Cx47Arg98Leu data. Dashed lines are Boltzmann fits to steady state Cx47WT/Cx47WT and Cx43WT/Cx47WT G_j-V_j relations.

Table 1

Junctional conductances (in nS) for Cx43WT (43WT), Cx47WT (47WT), Cx47Arg98Leu (R98L) and controls in homotypic and heterotypic configurations.

Cell pairings	n	Mean	Std. Deviation	Std. Error	P vs WT47/WT47	P vs iG/iG
47WTiG/47WTiG	13	42000	44000	12000	-	***
47R98LiG/47R98LiG	30	2100	8800	1600	***	ns
47WTiG/47R98LiR	15	3200	7000	1800	*	ns
47WTiG/47WTiR	6	41000	33000	14000	ns	**
47R98LiG/43WTiR	15	14000	26000	6600	ns	*
47WTiG/43WTiR	6	39000	19000	7700	ns	***
iG/iG	13	40.	110.	29	***	-

iG-pIRES EGFP; iR-pIRES dsRed;

* p<0.05,

** p<0.01,

*** p<0.001.

Table 2

Boltzmann parameters for fits to the Gj-Vj relations of the noted pairing configurations.

Parameter	47WT/47WT	47R98L/47R98L	43WT/47WT	43WT/47R98L
Gmin(+)	0.133	0.103	0.284	0.210
Gmax (+)	0.996	0.997	0.995	1.028
Vo (+)	46.7	44.0	50.3	51.4
A(+)	−0.170	−0.185	−0.127	−0.0849
Gmin(−)	0.142	0.0904	0.0558	0.0892
Gmax (−)	0.995	1.00	1.001	1.01
Vo (−)	−44.5	−43.0	−41.3	−47.4
A(−)	0.197	0.241	0.337	0.147

Parameters are as described in the Methods. (+) and (−) refer to the limb corresponding to positive or negative V_j. Cx43WT (43WT), Cx47WT (47WT), Arg98Leu (R98L).